Modeling the Effects of Corrosion on the Lifetime of Extended Reinforced Concrete Structures

Alberto A. Sagüés
Department of Civil and Environmental Engineering
University of South Florida
Tampa, Florida 33620, U.S.A.

ABSTRACT

A modeling approach is presented for quantitative projections of corrosion damage in the substructure of marine bridges, taking into account the compounded variability of concrete cover, chloride diffusivity, and chloride surface concentration. The projections reduce to a multiple integral when the mechanisms of both corrosion initiation and propagation are such that distress is always manifested first in elements with the lowest clear concrete cover. The projected damage functions reflected the dispersion of the assumed controlling model variables. Two examples of model application are presented. In the first case the deterioration of a dual bridge built with high quality concrete but low reinforcing steel cover was considered. For that case projected deterioration on much of the substructure was dominated by the corrosion initiation stage. The second case addressed the development of corrosion of epoxy-coated rebar on a family of bridges where chloride diffusivity was high and there was much variability in concrete cover. In this case the effect of concrete cover variability on the extent of the corrosion propagation period was introduced as well. Damage progression was found to be dominated by the development of the corrosion propagation stage. Application of the models to these two cases produced output consistent with observed behavior. However, absolute model forecasts are affected by uncertainty in inputs and basic assumptions. Modeling approaches such as those presented here are expected to be most useful when assisting in comparing design or rehabilitation alternatives, or as an aid in elucidating corrosion mechanisms. Areas for future improvement of this methodology include accounting for effective diffusivity and surface concentration variations with time, the effect of chloride ion binding on diffusion, the effect of rebar potential on corrosion threshold, and a more precise evaluation of the length of the corrosion propagation stage.

INTRODUCTION

Predicting damage progression with time (the "damage function") in reinforced concrete structures subject to steel corrosion damage is important to design and maintenance. Reliable methods for corrosion forecasting are especially desirable for service applications that involve exposure to chloride ions, which affects a large part of the worldwide transportation infrastructure. The task, however, is made complicated by the variability of exposure and materials conditions existing within even a small structure. This complication notably affects marine bridge substructure where chloride

transport regimes change dramatically with elevation above sea level. A general approach to corrosion damage forecasting under distributed conditions is presented here, together with two specific illustrations.

The progression of events leading to corrosion related damage in concrete may be summarized as follows. In normal Portland cement concrete made with uncontaminated water and non-aggressive admixtures or aggregates, the pore water solution contains mostly K^+, Na^+, Ca^{++} and OH^- ions (typically $12.5 < pH < 13.5$) [1], and dissolved O_2 from atmospheric exposure. Under those conditions the steel of a reinforcing bar (rebar) and other carbon steel components[a] embedded in concrete is in the passive condition, with effective corrosion rates $<<1$ μm/y [2]. However, in marine environments chloride ions are present at the external concrete surface due to contact with seawater. At low elevations above the high tide line evaporative accumulation can cause the concentration of chloride ions in the pore water at the surface of the concrete to approach values close to saturation. Inward flow of chloride ions takes place, mainly by diffusional transport driven by the concentration gradient between the external surface and the interior [3] (other processes, such as capillary suction, can be important as well). As a result, the chloride concentration at the steel surface increases slowly with time, eventually reaching a critical threshold value C_T for depassivation of the steel [4]. Active corrosion ensues, initially in the form of pits but afterwards more generalized as the chloride concentration continues to increase. Average corrosion rates are then dramatically higher (e.g. 10 μm/y) than in the passive regime [5]. The cathodic reaction in actively corroding steel in concrete is usually reduction of oxygen, which is transported to the steel surface by diffusion through the concrete cover [2].   Corrosion metal loss ultimately weakens the structure through loss of steel cross section and steel-concrete bond. However, concrete damage from expansive corrosion products becomes important much earlier especially under atmospheric exposure [3,5,6]. The products from chloride-induced corrosion are usually in the form of solid metal hydroxides with volume twice or more greater than the lost steel [7], thus having an effect similar to that from an increase in the diameter of the steel bars. As concrete has low tensile strength (e.g. only a few MPa) and very little ductility, corrosion-induced cracks develop that later cause concrete delamination and spalls. It is this form of damage that creates the most frequent demand for structural maintenance, which in a marine environment may involve very costly access to the substructure for repairs.

The simplest forecasting of corrosion deterioration in concrete involves a two-period approach [8]. In the first period or stage (initiation), the chloride ion concentration at the steel surface is initially below C_T. The initiation period ends when the chloride concentration at the rebar surface reaches the value C_T. Active corrosion ensues signaling the beginning of the propagation stage during which corrosion products accumulate.   The propagation period is considered to   end with the development of concrete cover delamination spalls, appearance of concrete cracks, or similar external manifestations of distress generally designated as "damage".

The length ti of the initiation period can be evaluated with appropriate information and assumptions on the mechanism of chloride transport and value of the transport parameters, and on the value of C_T. The length tp for the propagation period can be estimated from materials and environmental properties as indicated later, or assigned a nominal value based on prior experience. In a structural element with uniform concrete cover, concrete and rebar properties, and exposure conditions, the damage function would take the form of a step: damage is unobservable (or below

---

[a] Most rebars in common use are made of plain carbon, hypoeutectoid steel with a pearlitic microstructure and yield strength in the order of 0.4 GPa. Pre- and post-tensioned steel strands, also used in cementitious media, typically have closer to eutectoid compositions and thermomechanical treatments resulting in very high ultimate tensile strength (e.g ~1.8 GPa). Although the text in this paper refers primarily to rebar steel, much applies as well to other carbon steel components in concrete.

some acceptable limit) before ti + tp, and damage is observable (or exceeding some tolerable limit) afterwards. The element would then experience a sudden transition from not being considered damaged, to being declared as such. However, experience shows that in actual structures distress is observed (or exceeds a given limit) at different times for different elements within the structure, leading to gradual development of damage for the entire system. This behavior may be envisioned as resulting from the superposition of numerous individual step functions corresponding to the end of the propagation stage of different portions of the structure, each with its own values of chloride transport, corrosion initiation, and corrosion propagation parameters.

GENERAL APPROACH TO MODELING DISTRIBUTED BEHAVIOR

The main premise in the approach outlined here is that the structure exposed to corrosion risk can be divided into a large number of individual elements of equal size, traced on the concrete surface, such that the corrosion initiation and propagation processes within each element are independent of those in any other element. The element size is assumed to be small enough that the concrete and reinforcement properties, as well as the concrete cover and surface exposure conditions, may be considered to be uniform. On the other hand, the element size is assumed to be large enough that when corrosion propagates and damage is eventually made visible in the form of concrete cracking or delamination, the damage does not extend into neighboring elements.

Parameters of importance within each element to defining the length of the corrosion initiation stage may include properties such as C_T, the clear concrete cover x, the apparent chloride ion diffusivity D [3], and the chloride concentration at the concrete surface. On first approximation, these parameters can be used together with an assumption of simple Fickian diffusion to obtain an estimate of the value of ti as it will be shown below. Laboratory experiments and field investigations generally support the approximate treatment of chloride as a simple diffusional problem [9]. More refined approaches (not included in the case applications discussed later) can include variability of diffusivity with time [10], and the retarding effect on penetration of chloride by binding with cement hydration products [11]. The length tp of the propagation stage is sometimes assumed to be an approximately fixed value. This assumption stems from the observation in some systems (such as highway bridge decks [9]) of propagation stages that are normally short compared with the typical length of the initiation period. In those cases an accurate evaluation of tp is less important and a flat value is assumed instead. More sophisticated treatments take into consideration the effect of system variables on tp. For example, when the corrosion over a given length on the rebar is relatively uniform, cover cracking tends to be observed when the average corrosion penetration χ (with its associated volumetric expansion from corrosion products) on that length of the bar reaches a critical value χ_{CRIT}. For atmospheric exposure the value of χ_{CRIT} (which often is very small, e.g. 0.1 mm) is observed to increase with the ratio of x to the rebar diameter Φ [12]. Thus if the corrosion rate prevalent over a rebar segment during the propagation period does not depend strongly on time or on x, then χ increases linearly with time until reaching χ_{CRIT} and tp may be assumed to increase approximately linearly with x/Φ. A proportionality factor $k = tp\ \Phi/x$ was defined to implement such approximation in one of the Case Applications detailed below. In more detailed models, k may be also assigned a dependence on corrosion rate, or on the condition of the coating if rebar coated with epoxy is used. Modeling efforts for tp of much greater complexity (e.g. dealing with the transition from early pitting to more uniform corrosion) are not in common use at present.

If only the variables just considered were of importance, the total time to developing externally observable damage, ts, on an element could be expressed as

$$ts = f(x, D, Cs, C_T, \Phi, k) \tag{1}$$

If the values of all the parameters other than x were kept the same, then the value x_s of x that results in damage appearing at time ts $ tp could be expressed as a function of the other parameters such as:

$$x_s = F(ts, D, Cs, C_T, \Phi, k) \tag{2}$$

The actual form of functions f and F depends on the chloride transport, initiation and propagation models, and number of relevant variables assumed. Examples of those forms will be presented in the following sections.

For greater generality, a series of variables $V_1...V_n$ can be considered where $V_1=x$, and $V_2,...,V_n$ represent all the other relevant factors or parameters affecting corrosion initiation and propagation. Thus a more general form of Eqs. (1) and (2) is:

$$ts = f(V_1, ...Vn) \tag{3}$$

$$V_{1s} = F(ts, V2....Vn) \tag{4}$$

In an actual structure all these parameters are subject to variability that can be both systematic (for example decreasing Cs with elevation above sea level in marine bridge substructure) and probabilistic (such as changes in D with batch-to-batch variations in concrete mixture proportions [3], or with concrete placement quality). Thus, it will be assumed that the structure can be divided into separate regions (for example elevation ranges) such that within each range the values of variables $V_1...V_n$ obey independent probability distributions with parameters that depend on the region considered. In the following, regions will be numbered $1,2,...i....N_r$, and elements within each region will be numbered $1,2,...j...N_i$ [b].

Thus the probability that the value of parameter V_k in element j within region i is within an interval dV_k wide around the value V_{kij} is $P_{ki}(V_{kij}) dV_k$, where P_{ki} is the probability distribution function for variable V_k in elevation range i. As the probability distribution functions are assumed to be independent of each other within a given region, the probability of finding a combination of values (within specified intervals) of different parameters in a given element is simply the product of the individual probabilities. For a structure containing an arbitrarily large number of elements, the probabilities thus evaluated represent the fraction of elements having the specified combination of parameters.

It will be further assumed that both the mechanisms of corrosion initiation and propagation are such that, if all the other variables are constant, distress will always be manifested first in the element with the least concrete cover. This assumption is consistent with diffusional chloride ion transport through the concrete cover, and with the observation indicated earlier that generally less steel corrosion is required to cause cracking of the concrete when the concrete cover is smaller [12]. Consider now within region i a set of elements that may have variable values of parameter V_1 (the steel cover x), but that share the same values for the remaining parameters $V_2.....V_n$ within infinitesimal intervals $dV_2....dV_n$. Per the latest assumptions, at time ts (Eqs.(1-4)) any elements within that set having $V_1 \# V_{1s}$ will already have experienced distress. The fraction of elements in the set satisfying that condition is obtained by integrating the V_1 probability distribution up to V_{1s},

---

[b] Note that the symbol ti used to denote initiation time is unrelated to the counting variable i.

yielding $\int_0^{V_{1s}} P_{1i}(V_1)dV_1 = P_{cum1i}(V_{1s})$, the cumulative probability for V_{1s}. V_{1s} is in turn equal to $F(ts, V2,..V_n)$ per Eq.(4). Thus, the fraction of elements in region i that belong to this set and that have also experienced distress by time t is:

$$dN_i(t)/N_i = P_{cum1i}(F(t, V_2,..V_n)) P_{2i}(V_2) ...P_{ni}(V_n) dV_2 ...dV_n \qquad (5)$$

Integrating now over all the possible parameter values in each region and adding up the results of all regions yields the fraction $Ns(t)/N$ of elements over the entire structure that have experienced distress by time ts:

$$Ns(t)/N = (1/\sum_i N_i) \sum_i N_i \int_{V2}\cdots\int_{Vn} P_{cum1i}(F(t, V_2,..V_n)) P_{2i}(V_2)...P_{ni}(V_n) dV_2...dV_n \qquad (6)$$

Eq.(6) then represents the progression of corrosion distress in the structure as function of time, which can be projected if one has knowledge of the distributions P_{ki} and the function $F(ts, V_2...V_n)$. Application of this approach to actual systems with significantly different corrosion forecasting needs is illustrated in the following sections.

CASE APPLICATION I - ESCAMBIA BAY BRIDGES

Case Statement

The parallel twin Escambia Bay bridges were built in 1966 to span Escambia Bay near Pensacola, Florida. The water chloride content exceeds 10,000 ppm at times. A durability forecast based on a 1997 condition survey was conducted using a precursor of the general modeling approach introduced here [13,14]. This section uses those published findings, reformulated in terms of the general equations presented in the Introduction, as a case application example.

Each bridge is 4.1-km-long, with 223 substructure bents (piers). The bents in the higher elevations of the bridges are comprised of 268, 1.37-m diameter spin-cast circular "Raymond" piles with longitudinal prestressed cables and spiral wrap-around stirrup wires. Smaller diameter 0.91-m Raymond piles (1,218 in water) support the lower elevations of the bridges. Only the durability of these piles is considered here.

Evaluation of the bridges at age 31 years was conducted by Concorr Inc. [14]. The evaluation included visual observation, direct examination of reinforcement, electrochemical corrosion measurements, concrete cover measurements, and determination of chloride ion penetration profiles. No corrosion-induced damage or deterioration of the round piles was found. The clear concrete cover of the piles (average of 2.84 cm for 47 test spots and 2.64 cm for 14 test spots in the 0.91-m and 1.37-m piles, respectively) corresponded to the spiral stirrup wire. Electrochemical and chloride penetration tests were performed at three elevations corresponding to the tidal zone (TZ), about 0.15 m below high tide elevation (-0.15 m above high tide, (HT), the upper splash zone (US), about 0.75 m above HT for the 0.91-m (3-ft) piles and 1.2-m above HT for the 1.37-m piles, and the above-splash zone (AS), about 1.5 m above HT. Average nominal corrosion current densities from polarization resistance measurements were in the range normally associated with low or negligible corrosion rates of steel in concrete [5]. Chloride concentration profiles were obtained at 17 unbiased sampling locations in the three elevation regimes indicated above, showing that the chloride concentrations in the US and AS zones at the depth of the stirrup wire were below (but near), and in the TZ were above,

the values (e.g. ~ 1 kg of Cl⁻ ions per m³ of concrete) normally associated with the onset of active corrosion of steel in concrete [4].

The results of that survey indicated that the corrosion condition of the piles was very good, especially considering the high Cl⁻ content of the water, the bridge age, and the low concrete cover thickness. However, the chloride profile results suggested that corrosion initiation had possibly already started in the TZ and was likely in the near future for the US and AS zones.

Spatial Distribution And Deterioration Model

The bridge round-pile substructure was divided into three elevation regions designated by i=1(tidal, T); i=2 (lower splash, LS) and i=3 (combined upper splash and above-splash, US-AS). The LS range was introduced as an artificial intermediate range of average properties between those of the T and the LS-US ranges, to address a region of possible early deterioration. A minority of piles with surrounding cast-in-place concrete struts of high w/c ratio was treated conservatively as if the struts offered no resistance to chloride penetration. Each elevation region was assigned N_i surface elements $(1,2,...,j,...N_i)$ of equal area Ae. Ni included the elements of both twin bridges.

Each element j in range i was assumed to have a concrete rebar cover $x_{i,j}$. Chloride ions were assumed to be transported by near-flat geometry Fickian diffusion, with an apparent chloride ion diffusion coefficient D_{ij} invariant with time for each element. The surface chloride ion concentration of each element was also assumed to have a time-invariant value $Cs_{i,j}$. The native chloride content of the bulk concrete was assumed to be the same throughout the bridge and negligibly small for the purposes of this model. The chloride concentration threshold C_{Ti} was assumed to be the same for all the elements within each elevation region. Likewise, the corrosion propagation time was assumed to be the same, tp_i, for all elements within each elevation region i.

The above assumptions imply then that the ruling parameters for Eqs.(2-3) are: V_1=x; V_2= Cs; V_3=D; V_4=C_T; V_5=tp, of which only V_1, V_2 and V_3 are distributed while V_4 and V_5 are constants within each region. Under simple near-one-dimensional diffusion with constant surface concentration and negligible native content, the chloride concentration at depth x and time t is given by

$$C(x,t) = Cs\left(1 - erf\frac{x}{2\sqrt{Dt}}\right) \tag{7}$$

Therefore the condition to achieve corrosion initiation is $C(x,ts) = C_T$ which per Eq.(7) means then that the function f adopts the form:

$$ts = \frac{x^2}{4D\left(erf^{-1}\left(1 - \frac{C_T}{C_S}\right)\right)^2} + tp \tag{8}$$

or:

$$ts = \frac{V_1^2}{4V_3\left(erf^{-1}\left(1 - \frac{V_4}{V_2}\right)\right)^2} + V_5 \tag{9}$$

Likewise, the function F adopts the form

$$x = 2 \sqrt{D(ts - tp)} \ \mathrm{erf}^{-1}\left(1 - \frac{C_T}{C_S}\right)$$ (10)

(for t>tp)

Thus Eq.(6) for this case takes the form:

$$\frac{Ns(t)}{N} = \frac{1}{\sum_i N_i} \sum_i N_i \int_{Dli}^{Dhi} \int_{Csli}^{Cshi} P_{cumxi}\left(2\sqrt{D(ts_i - tp_i)}\ \mathrm{erf}^{-1}\left(1 - \frac{C_T}{C_S}\right)\right) P_{csi}(Cs)\ P_{Di}(D)\ dCs\ dD$$ (11)

where Dl_i, $Csli$ and Dh_i, Csh_i represent the lowest and highest values respectively of D and C_S in elevation range i.   The total projected damaged surface area S(t) in the substructure at age t is then:

$$S(t) = Ns(t)\ Ae$$ (12)

Model Implementation

To calculate the projected damage function the following input parameters were required for each elevation range i (except for Ae, which is global) and obtained as follows:

Ae: Chosen to be 0.1 m², representing typical expected repair patch sizes (same for all elevation ranges).

N_i: Obtained from Ae, pile quantities, dimensions, and the elevation range limits designated per Table 1. The top and bottom of the T and LS ranges, respectively, were at the HT level. The T range span reflected the typical tidal variation in Escambia Bay. The US+AS range started at the top of the LS range. Elevations higher than 1.8 m (6.0 ft) above HT were assumed to result in negligible corrosion development in the time frame of interest.

C_{Ti} :   Assumed to be M • CF at all three elevation ranges. CF is the cement factor of the concrete used in the piles (assumed to be 400 kg/m³) and M is a multiplier often assumed to be 0.004 for design purposes [23]. However, because of uncertainty in this parameter, three alternative cases A, B, and C were evaluated with M= 0.004, 0.008 and 0.012, (thus C_{Ti} = 1.6 kg/m³, 3.2 kg/m³ , and 4.8 kg/m³) respectively.

$Pcs_i(C_S)$,
$Pd_i(D)$,
$P_{cumCi}(x)$:
       These distribution functions were approximated by fitting the measured populations to ideal normal distributions (as a working assumption in absence of evidence to the contrary, and not inconsistent with the available data shown in Figures 2 and 3) truncated as appropriate. The

normal distribution is unknown, Each distribution required four parameters: mean, standard deviation, and upper and lower truncation limits.

For the C_S and D distribution functions, a concrete unit weight of 2,547 kg/m^3 was used to convert chloride concentrations from percent by weight of concrete to kg/m^3. Based on measurements at depths of $\approx$10 cm, the native chloride content was assumed to be $\approx$0.12 kg/m^3. Figure 1 shows the values of D and C_S as a function of elevation obtained by analysis of 17 extracted cores from both types of piles. There was no significant evidence of different trends for the two size piles. Both C_S and D tended to be higher in the T range than in the US and AS ranges. The results of the two latter ranges were not clearly differentiated and were consequently grouped together. Table 2 presents the average and standard deviation values of D and C_S for each of the two distinct groups thus identified. The populations of both groups (especially that for the Tidal regime) are small, so the standard deviation values can only be considered as nominal values. Nevertheless, at least for the US + AS regimes, there is reasonable approximation between an ideal normal distribution and the actual cumulative value counts, as shown in Figure 2. Nominal parameter values were assigned for the LS zone and listed in Table 2. These values were intermediate between those for i=1 and i=3 and chosen to follow, at an elevation of .15 m above HT, the general trends of Figure 1.

For the x distribution function, direct measurement of the concrete cover in both size piles yielded similar results, as shown in Table 3.   The spiral pitch based on design data is only $\approx$7.5 cm, resulting in a large amount of stirrup steel. It was then expected that the first corrosion-related damage requiring extensive repair will be from the spiral wires. Since the piles were precast it was assumed that close dimensional control existed, so the same values (overall average = 2.79 cm; standard deviation = 0.63 cm) were used for i = 1 to 3. No distinction was made between the two size piles. Figure 3 shows the cumulative distribution of stirrup cover values for the 0.91-m piles, compared with an ideal cumulative normal distribution having the average and standard deviations for those piles. The resolution of the field measurements was $\approx$6 mm. No values lower than 1.9 cm were recorded for any of the stirrup measurements in either size piles. In an ideal normal distribution with the parameters for Figure 3, 0.85% of the stirrup measurements (less than 1 in a field of 47 tests) would have been 1.27 cm or less. Thus, the absence of lower readings in the present sampling is not by itself statistically indicative that the concrete cover in the stirrups was limited by construction to 1.9 cm. However, some form of cover limitation (for example, by the use of form saddles) was likely in the precast procedure.   Moreover, corrosion damage was not conspicuous anywhere in the 1,486 piles on water after 31 years of service. Consequently for the purposes of the model, the distribution was truncated at 1.9 cm.

tp_i: In the absence of corrosion measurements of confirmed active steel, the value of tp_i for elevation ranges 2 and 3 was assigned to be 7 years (2.2 10^8 sec). Because of the apparent high concrete quality, this value was twice the nominal value used in previous estimates of durability for the general population of bridges in Florida [15], which was in turn based on typical values of tp reported for corrosion of rebar in bridge decks [16]. The value assigned to tp_i, in the T elevation range was 30 years (9.5 10^8 sec). This is a nominal value, based on the expectation of much lower corrosion rates in the tidal region where very slow oxygen transport is anticipated, and on the high humidity of that region which is thought to lessen the accumulation of solid corrosion products at the rebar surface.

Calculation And Model Output

The calculations were conducted with a numerical worksheet, where Equation (11) was discretized and implemented as a double summation with typically 20 terms. Additional terms yielded only minor changes in output. Figure 4 shows the model output for Cases A, B and C (C_T equal to 1.6, 3.2 and 4.8 kg/m^3, respectively). The sum of the amount of damage for elevation ranges i=1, i=2 and i=3 (total for the two bridges) is given in m^2 as a function of time. The damage within each of the three elevation ranges is illustrated for Case C.

The model outputs show a period of no significant corrosion damage followed by the gradual development of deterioration afterwards. The shape of the curves for each elevation range reflects the assumed dispersion of model parameters (concrete cover, surface concentration, and diffusivity) around their respective average values. As indicated in the Introduction, an assumption of no dispersion would have resulted in a sharp step damage function for each range, with damage starting at the time corresponding to that dictated by the average parameter values plus the assumed propagation time. The model outputs project the most damage taking place in the Tidal zone during the decades following the time of examination of the structures.

The projected bridge age for observation of significant corrosion was about 20 years for the most conservative of the alternative cases (C_T = 1.6 kg/m^3, Case A), and almost 40 years for the least conservative Case C. Thus, these alternatives bracket the observed absence of significant damage when the structures were examined at age 31. In all 3 realizations the total projected damage reached 1000 m^2 some 20 years after the first appearances of significant damage. Detailed cost estimates for rehabilitation were prepared and reported elsewhere [14] based on the repair/rehabilitation alternatives considered. It is emphasized that because of uncertainty in the input variables and model assumptions, the value of the output of this type of calculations is mainly as a means to compare the relative outcome of design or maintenance decisions than as an absolute prediction tool.

CASE APPLICATION II - FLORIDA KEYS BRIDGES BUILT WITH EPOXY COATED REBAR

Case Statement

As in the previous case, information from a previous study is used to illustrate the model formulation introduced here [17]. Epoxy-coated rebar (ECR) has been used in approximately 300 Florida bridges, principally in an attempt to control corrosion of the substructure in the splash-evaporation zone of marine bridges. The typically ~ 0.3 mm thick coating was applied in powdered form on freshly sandblasted rebar and heat-fused and cured. Starting in 1986, severe corrosion of ECR began to be observed in five major bridges built between 1978 and 1983 along US 1 in the Florida Keys. The characteristics and mechanisms of this form of corrosion have been discussed elsewhere [15,17,18]. The development of corrosion damage has been recorded periodically. Table 4 lists the structures affected, nomenclature, and construction information. Unless indicated otherwise, the concrete used in the substructure was cast in place (CIP) and conforming to FDOT Class IV specifications at the time of construction. Those specifications established w/c<0.41, cement content = 388 Kg/m^3, and 28-day strength >23.5 MPa. The fine aggregate was sand and the coarse aggregate oolitic limestone. The cement type for each structure is indicated in Table 4. The design clear rebar concrete cover for the substructure of these bridges was 76 mm. Substantial deviations from that

value were often observed, especially in round columns when the rebar cage was not precisely centered. As a result, it was not uncommon to encounter concrete cover as little as 25 mm on one side of the column and 125 mm on the other side. Some instances of no cover were encountered.

Initial chloride content of the concrete in the bridges was small (typically <0.24 kg/m^3) for NIL, LOK and CH5, but that it was considerably higher for 7MI (1.8 kg/m^3) and INK (0.7 - 2.1 kg/m^3). It has been speculated that the higher values reflected seawater contamination of the coarse aggregate.   The ECR had been manufactured and coated following ASTM 775 - 76 and ECR placement guidelines in place at the time of construction [19,20]. Those guidelines allowed a maximum of 2% unrepaired surface damage at rebar surface. The coating material and applicators for each bridge are listed in Table 4. Rebar sizes ranged from #3 (10 mm diameter) to # 8 (25 mm). Rebar tie wires, as revealed by direct examination, were bare steel.

Table 5 lists the results of bridge examinations performed between 1986 and 2000. If evidence of cracking or other distress was observed, the affected substructure element was tested by sounding with a hammer for evidence and extent of internal delamination. An area of delaminated concrete thus detected was designated as a concrete spall. A delaminated area which extended from an area found to be spalled in a previous inspection was designated as a progressive spall. Typical spalls affected a projected area of ~0.3 m^2 (~3 sq.ft.) on the surface of the concrete. The number of new spalls or progressive spalls observed on a bridge at a given inspection date was recorded. That number was then added to those observed in the previous inspections of the same bridge, and reported in Table 5 as the cumulative number of spalls to the listed date. Spalls that occurred in regions formerly repaired were considered a new spalls.

Chloride ion profiles indicated that extensive chloride penetration of the concrete had taken place in the splash zone of the structures affected. At the time of the first spall observations, chloride content at a depth of 50 mm to 76 mm in the splash zone of LOK, 7MI and NIL was between 8 kg/m^3 and 14 kg/m^3 [15]. The value of Cs typically reached ~14 kg/m^3 at the bottom of the splash evaporation zone and decreased with increasing elevation. D values determined from the chloride profiles for the splash zone in those bridges ranged from ~10^{-8} cm^2/sec to as much as ~6 10^{-7} cm^2/sec [15,21]. These high diffusivities agreed with concrete resistivity readings as low as ~1 kΩ cm in the tidal region [15,22].

Actual Corrosion Progression

To compare the progression of corrosion in bridges of different lengths, the data in Table 5 were normalized by dividing the number of spalls by the number of bents in each bridge.   The resulting damage functions (spalls per bent as function of time) are plotted in Figure 5. The corrosion damage after nearly 20 years of service is conspicuous (more than one spall per bent) and affects a significant fraction of the area of the splash zone of each bridge (the concrete surface area on the splash zone of a typical bent is ~ 20 m^2 while a typical spall affects ~0.3 m^2). Damage is likely to have been worse without the application of protective anodes. Except for an offset toward shorter times for NIL, the functions are remarkably similar to each other. The damage at present appears to increase approximately linearly with time.   If those trends were to continue, the total extent of damage would roughly double over the next 20 years of service. As repairs in marine substructure are very costly, corrosion would place a continuing and heavy repair and maintenance burden during the service life of these structures.

Deterioration Model

The appearance of the damage functions in Figure 5 clearly indicates that the development of damage was gradual and amenable to an interpretation based on distributed variables. The modeling approach introduced above was adapted to the present case for future behavior projection and also to provide insight on the factors responsible for damage development in the past. For simplicity, the impact of corrosion control procedures in the observed damage functions was ignored.

As will be shown below, the corrosion propagation stage in these structures appears to dominate much of the damage development. Consequently, a more refined approach than in the previous Section was used here to assign values to tp, taking into consideration the approximate dependence of tp on rebar cover thickness and diameter indicated earlier assuming that it applies not only for plain steel rebar but to ECR as well. In ECR the corrosion rate (averaged over the bar surface) is strongly influenced by the condition of the coating [23,24]. Thus ECR with substantial coating distress should corrode much faster than in the absence of imperfections. Accordingly, for modeling purposes the propagation time was expressed as tp = k' x, where k' = k / Φ is a parameter that becomes smaller as the extent of ECR coating distress increases (for simplicity Φ was assumed to be same for all the rebar in the affected regions). Under those conditions the value of ts is given by:

$$ \text{ts} \;=\; \frac{x^2}{4\,D\left(\text{erf}^{-1}\left(1-\dfrac{C_T}{C_S}\right)\right)^2} \;+\; k'\,x \tag{13} $$

and the function F adopts the form:

$$ x = -\frac{k'P}{2} + \frac{1}{2}\sqrt{k'^{\,2}\,P^2 + 4\,\text{ts}\,P} \tag{14} $$

$$ \text{where} \quad P = 4\,D\left(\text{erf}^{-1}\left(1-\frac{C_T}{C_S}\right)\right)^2 \tag{15} $$

Replacing F in Eq.(6) then yields the corresponding damage function for the fraction of the surface having a given value of k'.

Input Parameters

As in the previous application, precise knowledge of the input parameters relevant for damage development in these structures is not available. However, insight on the factors responsible for the corrosion progression was sought by assuming parameter values and variability (Table 6) consistent with the information detailed in the case statement. Thus, a mean D on the order of $2\ 10^{-7}$ cm^2/sec was assumed. The spatial distribution of C_S was approximated by a normal distribution truncated at a nominal mean value of 14 kg/m^3. The design value of x (76 mm), and the range of

variation of x (0 to 160 mm), are known from specifications and can be estimated from field observations respectively. Variability in the values of x, D and C_S was idealized as before by normal distributions, with a standard deviation equal to ¼ of the mean, and truncated as appropriate. Laboratory observations suggest that under simple conditions C_T for ECR is on the order of the value for plain steel bar [18]. Thus, a single case with C_T ~0.004 CF (the middle of the three choices investigated in the previous Section) was assumed. Variability in tp was introduced in the model through the parameter k', an approach that produced plausible results when used together with the value of C_T used.

Calculation And Model Output

The calculations assumed initially chloride-free concrete. The assignment of k' values over the rebar assembly, which was treated for simplicity as a discrete distribution, assumed that only a small fraction (2%) of the rebar assembly was responsible for the earliest observations of damage. That fraction had a low value of k' (0.14 y/mm, which results in tp=7 years when x=50 mm) and consequently was responsible for the very first failures projected. Increasingly large fractions of the assembly were assumed to have correspondingly larger propagation times. This approach is based on the expectation that rebar segments with a high incidence of coating distress are likely to have the highest corrosion rates and therefore the shortest tp values. The chosen distribution for k' then effectively states that there was a small fraction of the rebar with severe coating distress, and proportionally less distress on increasing fractions of the assembly. Figure 6 shows the model output. The effect of the model assumptions is apparent in the dashed lines of Figure 6, which show the contribution to the total damage from each of the distress fractions assumed.

The choice of input parameters used yielded a projected damage evolution for the first 20 years that was consistent with the observed behavior in Figure 5. The projection reasonably reproduced the duration of the initial period with minimal damage, and the subsequent steady rise at a rate of ~0.1 spall/bent/year observed in the bridges. Sensitivity tests showed that the damage projection was only modestly influenced by changes in the distribution of D or C_S, or by variations in C_T. This behavior is a consequence of the severe exposure regime assumed, which causes the corrosion threshold to be reached at much of the rebar surface very early in the simulation. A similar circumstance may account in the actual structures for the little differentiation (Figure 5) between the trends in 7MI and INK, which had initial chloride contamination, and that of the other bridges. Thus the projected behavior was determined mainly by the corrosion propagation phase, which depended strongly on the k values and cover distribution assumed. It was felt that the chosen value for the variability of x (described by the parameter sx in Table 6) was reasonably representative as it allowed for ~10% of the cover to be less than 5 cm, reflecting several observations of low cover during inspection of the first recorded spalls. The k' distribution chosen for Table 3 was only a working example. However, ranging calculations confirmed that reasonable fit to observed behavior could be obtained only if the percentage of the assembly assigned low k' values (yielding tp values of only a few years) was quite small.

While exploratory in nature, the model projections for these bridges provide insight as to possible future behavior if the actual systems. As shown in Figure 6, as time progresses the projected damage is dominated by fractions with increasingly greater k'. Whether future damage will continue along the present trend depends, in this scheme, on the extent of coating distress on the rest of the rebar assembly. If the remaining rebar coating were in very good condition, damage would continue for some time at the present rate and then saturate at some intermediate level. In the case of the values assumed for Table 3, there was no k' value assigned beyond the first 14% of the rebar assembly, and damage would saturate at ~9 spalls per bent. If the condition of the remaining rebar were poor or marginal, damage progression would not saturate soon, and could even accelerate.

DISCUSSION

The benefits of a distributed parameter treatment for projections of corrosion in concrete have been apparent from previous investigations [9,21,25]. The treatment presented here provides a unified projection method that reduces to evaluating a multiple integral when the mechanisms of both corrosion initiation and propagation are such that distress is always manifested first in elements with the lowest clear concrete cover. The method was successfully applied to quantitative projections of future deterioration, or interpretation of historical damage development, involving major structures and taking into account the compounded variability of concrete cover, chloride diffusivity, and chloride surface concentration in the substructure of marine bridges. The ability of the treatment to include added functionality was demonstrated by the incorporation of dependence of propagation time on concrete cover in the model for the structures built with ECR. The projected damage functions effectively reflected the dispersion of the assumed controlling model variables. The case applications provided quantitative projections that, while not intended as absolute prediction tools, permitted comparing repair and future construction alternatives for decision-making (e.g. Escambia Bay Bridges), or provided understanding on the mechanisms of deterioration in action as well as evaluation of future maintenance needs (bridges with ECR). For those purposes, the modeling approach presented here represents a significant improvement over analyses based on the behavior of single elements with a simple step damage function [32].

The case applications underscored that significant uncertainty comes from imprecise knowledge of input variables and of the processes at work. In some instances, it is difficult to discern between actual variability and measurement uncertainty in the main parameters (concrete cover, diffusivity, surface concentration) that were used as distributed values. However, the case applications also showed that the modeling methodology is well suited for rapid examination of the durability impact of changes in key variables such as C_T. Because of its generality, the model formulation is capable also of expansion to include additional sophistication. Notable issues that can be incorporated in the model to advantage include the possibility of alternative C_T regimes for ECR as reported elsewhere [21], effective diffusivity and surface concentration variations with time [10,26], the effect of chloride ion binding on diffusion [11], alternative chloride transport mechanisms [27], and especially the effect of rebar potential on C_T [28,29]. The latter could be especially important in the ECR bridges case as concrete resistivity there tends to be low [15,18], leading to efficient coupling of still passive steel with nearby anodic regions [2,18]. Such coupling could lead to substantial elevation of the value of C_T of the passive steel [28-30] with consequent retardation of corrosion initiation and dramatic alteration of the calculated the damage projection. In that case, model reformulation is needed to include interaction between adjacent surface elements that are no longer independent. Next generation models are beginning to address those issues, as well as incorporating the effect of corrosion protection measures such as sacrificial anodes [31,32].

CONCLUSIONS

1. Quantitative projections of future deterioration and interpretation of historical damage development can be performed by taking into account the compounded variability of concrete cover, chloride diffusivity, and chloride surface concentration in the substructure of marine bridges. The projections reduce to a multiple integral when the mechanisms of both corrosion initiation and propagation are such that distress is always manifested first in elements with the lowest clear concrete cover. The projected damage functions reflected the dispersion of the assumed controlling model variables.

2.   Application of the models to two cases of corrosion in marine bridges produced output consistent with observed behavior. However, absolute model forecasts are affected by uncertainty in inputs and basic assumptions. Modeling approaches such as those presented here are expected to be most useful when assisting in comparing design or rehabilitation alternatives, or as an aid in elucidating corrosion mechanisms.

3.   Areas for future improvement of this methodology include accounting for effective diffusivity and surface concentration variations with time, the effect of chloride ion binding on diffusion, the effect of rebar potential on corrosion threshold, and a more precise evaluation of the length of the corrosion propagation stage.

ACKNOWLEDGMENTS

REFERENCES

[1]   Li, L., Sagüés, A.A. and Poor, N., **Cement and Concrete Research**, Vol. 29, p.315, 1999.

[2]   Sagüés, A.A.,   Pech-Canul, M..A. and Al-Mansur, S., **Corrosion Science**, Vol.45, p.7, 2003

[3]   Bamforth, P. B., "The Derivation Of Input Data For Modelling Chloride Ingress From Eight-Year UK Coastal Exposure Trials", **Magazine of Concrete Research**, Vol. 51, p.87, 1999.

[4]   Li, L. and Sagüés, A.A., **Corrosion**, Vol. 57, p.19, 2001.

[5]   Andrade, C. and Alonso, C., "Values of Corrosion Rate of Steel in Concrete in Order to Predict Service Life of Concrete Structures", in "Application of Accelerated Corrosion Tests to Service Life Prediction of Materials", STP 1194, G. Cragnolino, Ed., ASTM, Philadelphia, 1992.

[6]   Bentur, S. Diamond, N.S. Berke, "Steel Corrosion in Concrete: Fundamental and Civil Engineering Practice", E & FN Spon, New York, 1997.

[7]   Mehta, P. "Concrete, Structure, Properties and Materials", Prentice-Hall, Englewood Hills, New Jersey, 1986.

[8]   Tuutti, K., "Corrosion of Steel in Concrete" (ISSN 0346-6906), Swedish Cement and Concrete Research Institute, Stockholm, 1982.

[9]   Cady, P.D., and Weyers, R.E., **Journal of Transportation Engineering**, American Society of Civil Engineers, Vol. 110, No. 1, January 1984, pp. 35 - 44.

[10] Mangat, P., and Molloy, B., **Materials and Structures**, Vol. 27, p.338-346, 1994.

[11] Tang, L., **Cement and Concrete Research**, Vol. 29, p. 1463 (1999)

[12] Torres-Acosta, A.A., and Sagüés, A.A., "Concrete Cover Cracking with Localized Corrosion of the Reinforcing Steel", p. 591 in Proc. of the Fifth CANMET/ACI Int. Conf. on Durability of Concrete, SP-192, V.M Malhotra, Ed., American Concrete Institute, Farmington Hills, Mich., U.S.A., 2000.

[13] Sagüés, A.A., Scannel, W. and Soh, F.W., "Development of a Deterioration Model to Project Future Concrete Reinforcement Corrosion in a Dual Marine Bridge", in Proc. International Conference on Corrosion and Rehabilitation of Reinforced Concrete Structures, Orlando, FL, Dec. 7-11, 1998, CD ROM Publication No. FHWA-SA-99-014, Federal Highway Administration, 1998.

[14] Scannel, W., Soh, F., Sohanghpurwala, A. A., and Sagüés, A., "Assessment of Rehabilitation Alternatives for Bridge Substructure Components" Final Report, CONCORR, Inc., Ashburn, VA, 1998.

[15] Sagüés, A.A., "Corrosion of Epoxy-Coated Rebar in Florida Bridges", Final Report to Florida D.O.T., WPI No. 0510603, May, 1994, available from Florida Department of Transportation, Research Center, Tallahassee, Florida.

[16] Weyers, R.E., Prowell, B.D., Al-Qadi, I.L., Sprinkel, M.M., Vorster, M., " Concrete Bridge Protection, Repair, and Rehabilitation Relative to Reinforcement Corrosion: A Methods Application Manual", SHRP-S-360, Washington, DC:National Research Council, 1993.

[17] Sagüés, A.A., Powers, R.G., and Kessler, R., "Corrosion Performance of Epoxy- Coated Rebar in Florida Keys Bridges", Paper 06142, Corrosion/2001, NACE International, Houston, TX, 2001.

[18] Sagüés, A.A., Perez-Duran, H.M., and Powers, R.G., **Corrosion**,Vol. 47, No. 11, p. 884, 1991.

[19] Sagüés, A., Powers, R. and Kessler, R., "Corrosion Processes and Field Performance of Epoxy-Coated Reinforcing Steel in Marine Substructures", Paper No. 299, Corrosion/94, NACE International, Houston, 1994.

[20] Sagüés, A. and Powers, R. "Coating Disbondment in Epoxy-Coated Reinforcing Steel in Concrete - Field Observations", Paper No. 325, Corrosion/96, NACE International, Houston, 1996.

[21] Hartt, W., Lee, S.K., and Costa, J., "Condition Assessment and Deterioration Rate Projection for Chloride Contaminated Concrete Structures" p.82 in Repair and Rehabilitation of Reinforced Concrete Structures: The State of the Art, Silva-Araya, W.P., de Rincon, O. T., and Pumarada O'Neill, L., Eds., ASCE, Reston, VA, 1998.

[22] Berke, N.S., and Hicks, M.C., "Estimating the Life Cycle of Reinforced Concrete Decks and Marine Piles using Laboratory Diffusion and Corrosion Data", p. 207 in Corrosion Forms and Control for Infrastructure, ASTM STP 1137, Victor Chaker, Ed., ASTM, Philadelphia, 1992.

[23]   Clear, K.C., **Concrete International**, p. 58, Vol. 14, May 1992.

[24]   McDonald, D.B, Pfeifer, D.W. and Sherman, M.R, "Corrosion Evaluation of Epoxy-Coated, Metallic-Clad and Solid Metallic Reinforcing Bars in Concrete", Report No. FHWA-RD-98-153, Nat. Tech. Info. Service, Springfield, VA, 1998.

[25]   Weyers, R., "Corrosion Service Life Model Concrete Structures", p.105, in Repair and Rehabilitation of Reinforced Concrete Structures: The State of the Art, Silva-Araya, W.P., de Rincon, O. T., and Pumarada O'Neill, L., eds, ASCE, Reston, VA, 1998.

[26]   Thomas, M.D.A. and Bentz, E.C. "Life 365 – Computer Program For Predicting The Service Life And Life-Cycle Costs Of Reinforced Concrete Exposed To Chlorides", distributed by The Concrete Corrosion Inhibitors Association, 2000.

[27]   Dihr, R., Jones, M., Byars, E., and Shaaban, I., "Predicting concrete durability from its absorption", p. 1177, in "Durability of Concrete", Malhotra, V., Ed., SP 145, ACI, Detroit, 1994.

[28]   Presuel-Moreno, F.J., Sagüés, A. A., and S.C. Kranc, "Steel Activation in Concrete Following Interruption of Long Term Cathodic Polarization", Paper #02259, Corrosion/2002, NACE International, Houston, 2002.

[29]   Alonso, C., Castellote, M. and Andrade, C., **Electrochimica Acta**, Vol. 47, p. 3469, 2002.

[30]   Pedeferri P., "Cathodic Protection and Cathodic Prevention", **Construction and Building Materials**, Vol. 10, p. 391, 1996.

[31]   Sagüés, A.A. and Kranc, S.C. "Model for a Quantitative Corrosion Damage Function for Reinforced Concrete Marine Substructure" in Rehabilitation of Corrosion Damaged Infrastructure, p.268, Proceedings, Symposium 3, 3rd. NACE Latin-American Region Corrosion Congress, P.Castro, O.Troconis and C. Andrade, Eds., ISBN 970-92095-0-7, NACE International, Houston, 1998.

[32]   Sagüés, A. and Powers, R., **Corrosion**, Vol. 52, p.508, 1996.

TABLES

Table 1 – Elevation Ranges and Elements for Escambia Bay Bridges[13]

Piles	Number in water	Perimeter (m)	Range Height (m)			Range Area, Both Bridges (m^2)		
			T i=1	LS i=2	US+AS i=3	T i=1	LS i=2	US+AS i=3
0.91-m	1218	2.87	0.45	0.3	1.5	1573	1049	5243
1.37-m	268	4.31	0.45	0.3	1.5	520	347	1733
			Both Piles (m^2) :			2093	1395	6976
			Number of elements for Ae = 0.1 m^2, Both Piles (N$_i$)			20928	13952	69761

Table 2 – Escambia Bay Bridges Parameters[13]

	TIDAL (i=1)	D(in^2/y)	Cs(%)	D(m^2/s)	Cs(kg/m^3)
T i=1	AVG:	1.04e-02	0.98	2.13e-13	25.02
	STDEV:	7.0e-03	0.47	1.4e-13	12.1
LS* i=2	AVG:	5.00e-03	0.60	1.0e-13	15.3
	STDEV:	2.5e-03	0.30	5.1e-14	7.6
US+AS i=3	AVG:	2.42e-03	0.385	4.95e-14	9.80
	STDEV:	1.3e-03	0.20	2.6e-14	5.2

*assigned values

Table 3 – Positions Tested, Escambia Bay Bridges[13]

Pile	Number or test spots	Strands				Stirrups			
		Avg (cm)	St. Dev. (cm)	Highest (cm)	Lowest (cm)	Avg (cm)	St. Dev. (cm)	Highest (cm)	Lowest (cm)
0.91-m	47	4.04	1.12	5.71	2.54	2.84	0.66	5.08	1.90
1.37-m	14	3.51	1.24	5.08	1.27	2.64	0.51	3.17	1.90

Table 4 – Florida Keys Bridges[17]

BRIDGE	7 MILE (7MI)	NILES CHANNEL (NIL)	LONG KEY (LOK)	INDIAN KEY (INK)	CHANNEL #5 (CH5)
FDOT Bridge Number	900020	900117	900094	900095	900098
Year Built	1980	1982	1980	1981	1981
Number of Bents	264	38	102	19	35
ECR Source	Florida Steel	Bethlehem Steel	Florida Steel	Bethlehem Steel	Bethlehem Steel
Epoxy Coating Powder	Scotchkote 213	Scotchkote 213	Scotchkote 213 Hysol	Scotchkote 213	Scotchkote 213
Coating Applicator	Rezcom (Drilled Shafts) Santa Fe	Lane Metals MCP	Rezcom	MCP Lane Metals	MCP
Cement Type	II	II and III	I and III	II	III
Initial Concrete Cl$^-$ Content (kg/m^3)	1.7	0.15	0.15	0.65 - 2.1	0.15

Table 5 - Cumulative Spall Numbers Observed To Date Of Inspection, Florida Keys Bridges[17]

BRIDGE	7 MILE (7MI)	NILES CHANNEL (NIL)	LONG KEY (LKY)	INDIAN KEY (INK)	CHANNEL #5 (CH5)
Year Built	1980	1982	1980	1981	1981
Number of Bents	264	38	102	19	35
INSPECTION DATE			CUMULATIVE NUMBER OF SPALLS		
1986			1		
1987			3		
1988	8	17	17		
1989	22				
1990	58	34	45	2	
1993 (1st)					2
1993 (2nd)	175	54	83	10	18
1995	204	67	90	16	
1996	232			16	37
1998	290	81	123	23	47
1999	324				
2000	452				58

Table 6 – Calculation Parameters, Florida Keys Bridges[17]

A_f	Surface area of bent exposed to severe corrosion	20 m^2
A_e	Typical spall area	0.3 m^2
C_T	ECR chloride concentration threshold	1.55 kg/m^3
C_S	Average surface chloride concentration	14 kg/m^3
scs	Standard deviation of surface chloride concentration	$C_S/4$
C_{Smax}	Maximum surface chloride concentration	14 kg/m^3
x	Average rebar cover	76 mm
sx	Standard deviation of rebar cover	x/4
D	Average apparent chloride diffusion coefficient	2 10^{-7} cm^2/sec
sd	Standard deviation of app. diff. coeff.	D/4
k'	Proportionality constant for propagation time (Percentages indicate fraction of the surface assigned to the value).	0.14 y/mm (2%); 0.28 y/mm (4%); 0.56 y/mm (8%).

Note: C_S, x and D were assumed to be distributed as in a standard distribution, but truncated by zero and as shown by C_{Smax}, and normalized accordingly.
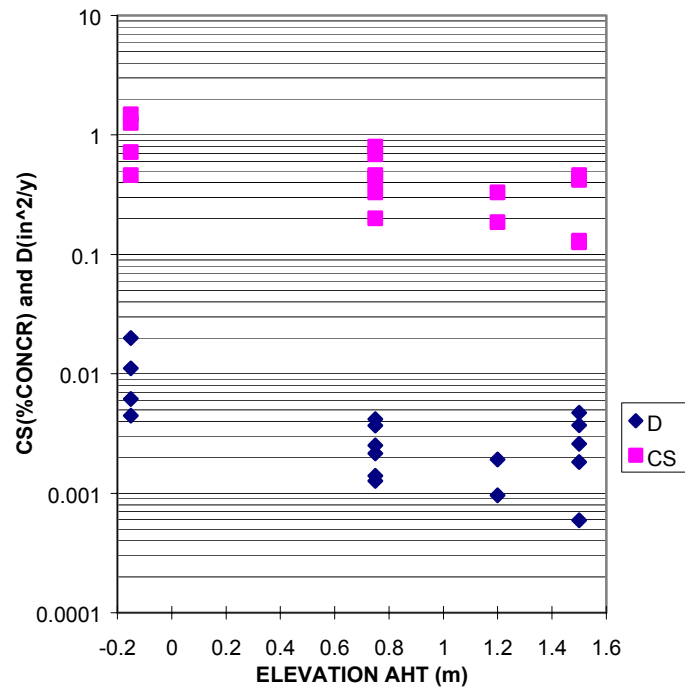
Figure 1. D and C_S as a function of elevation [13].
1 in^2/y = 2.05 10^{-7} cm^2/s.
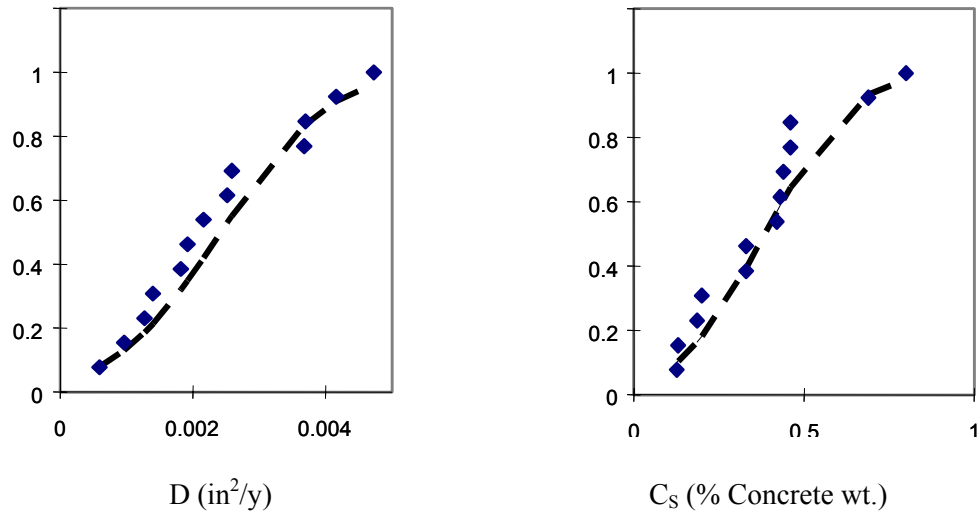1% of concrete weight = 25.5 kg/m^3.

D (in²/y)   Cs (% Concrete wt.)

Figure 2. Cumulative normal distributions (dashed lines) based on the average and standard deviation values in Table 2 for D and C_S in elevation ranges 2 and 3, and actual distribution of values [13]. 1 in^2/y = 2.05 10^{-7} cm^2/s. 1% of concrete weight = 25.5 kg/m^3.
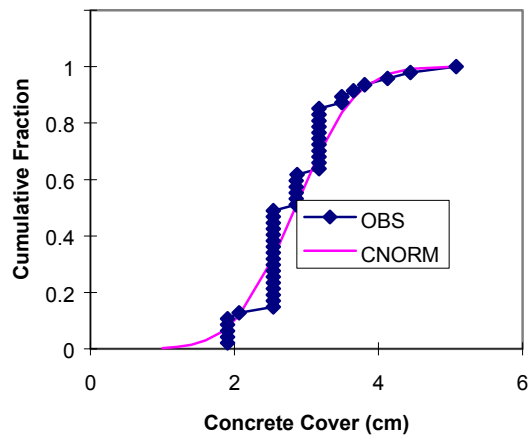
Figure 3. Cumulative normal distribution (CNORM) of stirrup concrete cover and observed values (OBS) for the 0.91-m piles [17].
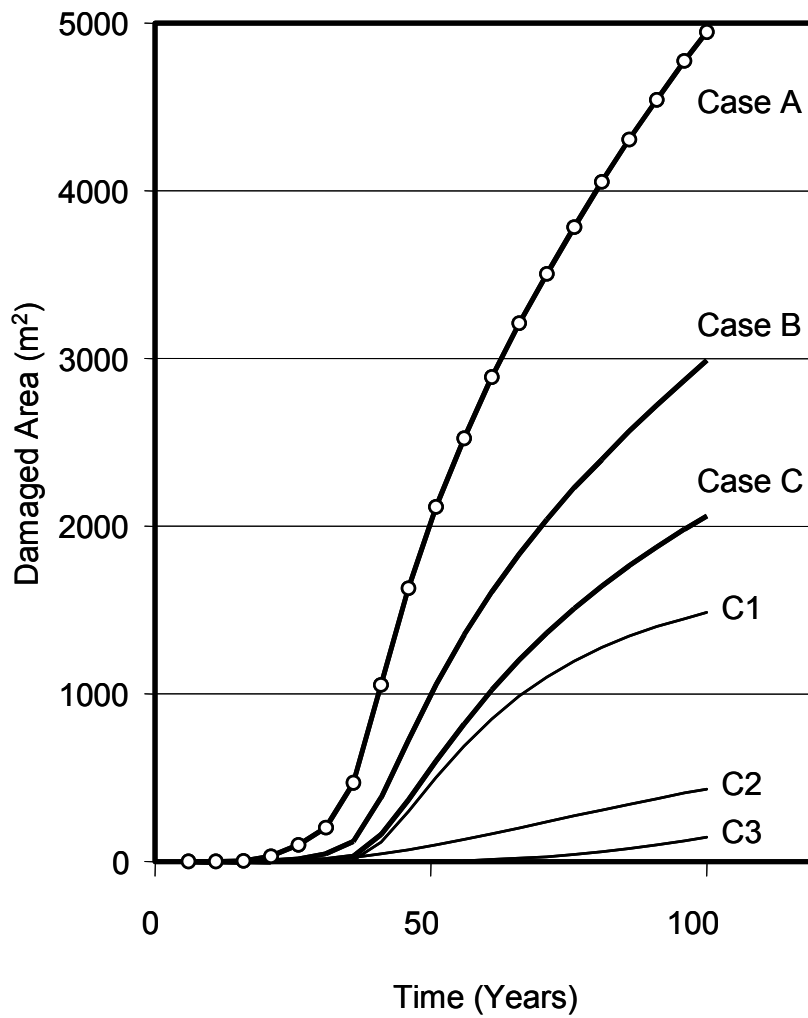
Figure 4. Model output for the Escambia Bay Bridge calculations[13]. The thick solid lines show the sum of the damaged areas in elevation ranges i=1 (T), i=2 (LS) and i=3 (US+AS) as function of time for each of the three alternative C_T Cases (A: $C_T = 1.6$ kg/m^3; B: $C_T = 3.2$ kg/m^3 ; C: $C_T = 4.8$ kg/m^3). Periodic calculation steps are illustrated by the circles for Case A. The thin lines labeled C1, C2 and C3 illustrate total damage for elevation ranges 1, 2 and 3 respectively in Case C.
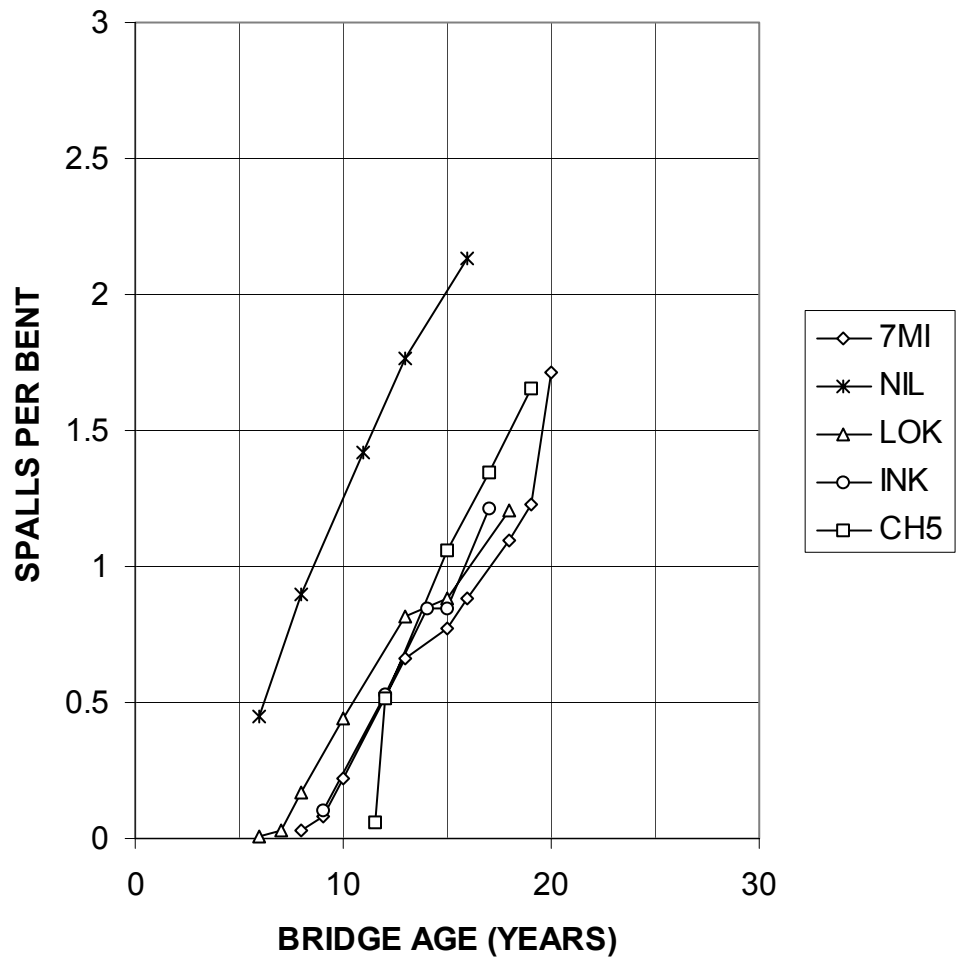
Figure 5. Progression of corrosion as function of time. Data from Table 5 were normalized by dividing by the number of bents (piers) in each bridge [17].
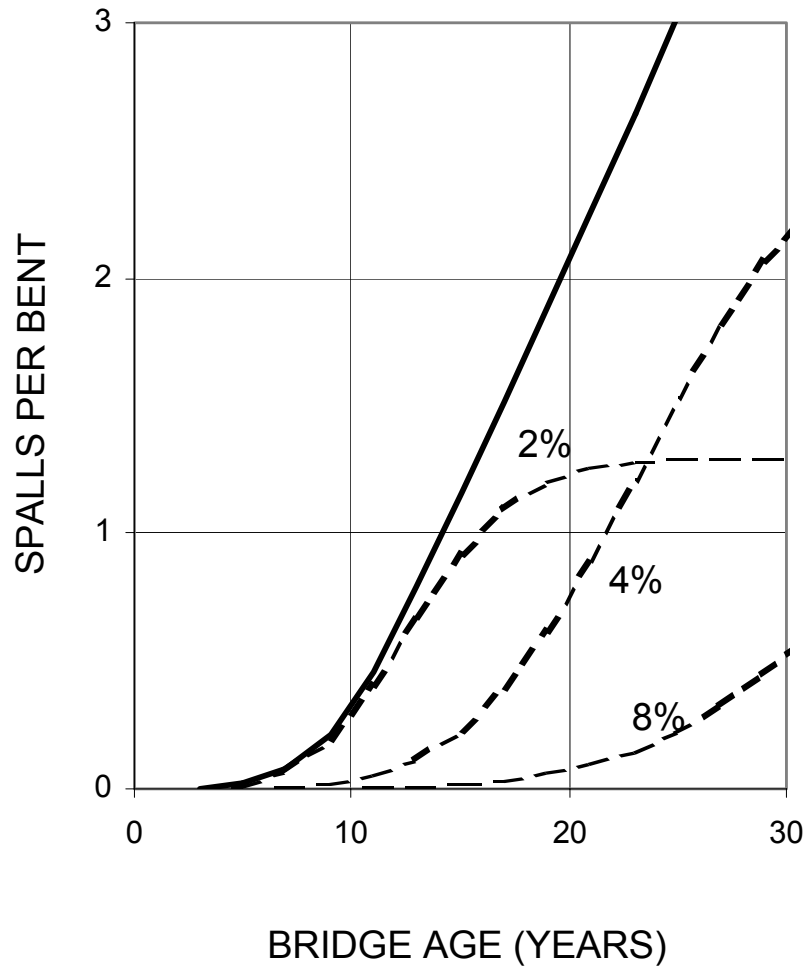
Figure 6 - Illustration of a projected damage function generally replicating the features and values of the behavior in Figure 7. The solid line corresponds to the total damage projection. The dashed lines correspond to the partial damage from each of the rebar assembly fractions considered: 2% of the rebar with k'=0.14 y/mm; 4% with k'=0.28 y/mm and 8% with k'=0.56 y/mm. Adding up the partial damages yields the total damage [17].